EUROPHYSICS LETTERS 1 September 1996

Europhys. Lett., **35** (7), pp. 499-504 (1996)

Energy loss of swift H_3^+-molecule ions in carbon foils

C. Denton[1], F. J. Pérez-Pérez[1], I. Abril[1], R. Garcia-Molina[2] and N. R. Arista[3]

[1] *Departament de Física Aplicada, Universitat d'Alacant*
Apartat 99, E-03080 Alacant, Spain
[2] *Departamento de Física, Universidad de Murcia - Apdo. 4021, E-30080 Murcia, Spain*
[3] *Instituto Balseiro, Centro Atómico Bariloche - RA-8400 Bariloche, Argentina*

(received 20 March 1996; accepted in final form 8 July 1996)

PACS. 34.50Bw – Energy loss and stopping power.
PACS. 36.40−c – Atomic and molecular clusters.

Abstract. – The energy loss of H_3^+-molecule beams interacting with amorphous carbon targets has been calculated, both as a function of the target thickness and the projectile velocity. We have considered the spatial changes, due to Coulomb repulsion, of the initial molecular configuration after the H_3^+ ion enters the target and then used a dielectric formalism to evaluate the stopping power of the correlated protons. The ratio between the stopping power of the H_3^+ molecule and that of its constituents considered individually accounts for the vicinage effects and agrees reasonably well with available experimental data.

Introduction. – Fast charged particles are widely used in physics to study and/or modify the structure of matter [1]. Recently, when molecular beams became easily available, a renewed interest in this subject has arisen [2], both for practical reasons (like possible applications in inertial-confinement fusion [3]), as well as from the theoretical point of view (to understand the differences that appear when a single charge or when an ensemble of charges with a well-defined geometrical structure —a molecule— interacts with matter). The energy loss of a molecular beam shows important differences (called vicinage effects [4]) with respect to the energy loss of its constituents independently considered. The origin of this effect lies in the manner in which the interference of the electronic excitations induced in the target by the swift charges affects the correlated motion of the particles that compose the molecule. The vicinage effect depends both on the kind of molecule (geometrical configuration, mainly), on its velocity, and also on the target properties.

Many papers have been devoted to study the interaction of molecular beams with matter, both experimentally and theoretically. Since the pioneering article of Brandt *et al.* [4], who studied the stopping power of swift molecules in solids, a lot of theoretical work has been developed [5]-[13]. Experiments have been mainly done with hydrogen-molecular ions, H_n^+, ranging from small [14]-[18] to intermediate [19] values of n.

In this work we use a dielectric formalism [5] to evaluate the stopping power of the correlated protons that form the H_3^+ molecule, and, simultaneously as the molecule travels through the

target, we take into account the spatial evolution of the initial molecular configuration, due to the Coulomb repulsion between the protons that occurs after the molecule enters the target and loses its binding electrons. The stopping power ratio, defined as the stopping power of the H_3^+ divided by three times the stopping power of a single proton with the same velocity as the molecule, compares fairly well with available experimental data [19] and Monte Carlo simulations [10].

Model. – When a fast H_3^+ molecule enters a solid, its binding electrons are quickly stripped off in the first atomic layers of the target [20]. Then the three protons of the molecule experience two different processes: electronic interaction with the target electrons and Coulomb repulsion due to their partners. In a first approach, these two processes can be thought as independent due to their different time scales [6]. This allows the evaluation of the molecule instantaneous-energy loss as a function of the internuclear separation, which changes with time due to Coulomb repulsion. The final observable energy loss of the molecule after traversing the foil is the averaged instantaneous-energy loss over the dwell time. Following this procedure for each incident-molecule energy, we will finally obtain the stopping power of the H_3^+ molecule as a function of the target thickness; dividing this quantity by the stopping power of three independent protons we obtain the so-called stopping ratio, which accounts for the vicinage effects that gives us information about the collective effects that take place due to the correlated motion of the protons in the molecule, as compared to the motion of three otherwise independent protons.

When the projectile velocity is larger than the Fermi velocity of the target electrons the energy loss is dominated by electronic processes, then nuclear energy loss can be neglected. The energy loss due to electronic interactions is described within the dielectric formalism [5], whose main ingredient is the dynamic response of the target electrons to external perturbations, described by the target dielectric function $\epsilon(k,\omega)$; k and ω represent, respectively, the momentum and energy of the target electronic excitations. Atomic units ([1]) will be used throughout this paper. The protons in the H_3^+-molecule ion form an equilateral triangle [21], with internuclear distance r, as the inset in fig. 1 shows. In this scheme and taking into account the interference effects felt by the protons in a molecule, the instantaneous stopping power of a H_3^+ molecule randomly oriented with respect to its velocity depends on the internuclear separation and is given by [5]

$$S_{H_3^+}(r) = \left[\sum_{i=1}^{3} Z_i^{*2} + \sum_{i\neq j}^{3} Z_i^* Z_j^*\, I(r)\right] S_p\,, \tag{1}$$

where Z_i^* is the effective charge of each proton in the molecule; we assume that the equilibrium charge state is reached for each constituent of the molecule and this means that the equilibrium charge state, or effective charge, is considered equal for atomic and molecular ions. At the velocities corresponding to the experimental situation to be compared with, the proton effective charge Z_p^* is close to unity [22], then $Z_i^* = Z_p^* = 1$. The proton stopping power S_p is given by

$$S_p = \frac{2}{\pi v^2}\int_0^\infty \frac{\mathrm{d}k}{k}\int_0^{kv} \mathrm{d}\omega\,\omega\,\mathrm{Im}\Big[\frac{-1}{\epsilon(k,\omega)}\Big]\,. \tag{2}$$

The interference function, $I(r)$ in eq. (1), accounts for the collective effects that appear in the

([1]) Atomic units are defined by the condition $m_e = e = \hbar = 1$, where m_e is the mass of the electron and e is the elementary charge.

stopping power of correlated particles and is written as [5]

$$I(r) = \frac{2}{\pi v^2 S_{\rm p}} \int_0^\infty {\rm d}k \, \frac{\sin kr}{k^2 r} \int_0^{kv} {\rm d}\omega \, \omega \, {\rm Im}\Big[\frac{-1}{\epsilon(k,\omega)}\Big] \, . \tag{3}$$

As we shall compare our calculation with experiments done on carbon foils [19] we model the dielectric properties of an amorphous carbon target by a sum of two Mermin-type energy loss functions [23] that, at zero momentum transfer, fits the experimental energy loss function:

$${\rm Im}\left[\frac{-1}{\epsilon(k=0,\omega)}\right]_{\rm experimental} = \sum_{i=1}^{2} A_i \, {\rm Im}\left[\frac{-1}{\epsilon_{\rm M}(\omega_i,\gamma_i;k=0,\omega)}\right] , \tag{4}$$

where $\epsilon_{\rm M}$ is the Mermin dielectric function [24], and ω_i and γ_i are related to the position and width of each peak in the energy loss spectrum. The coefficients A_i are determined under the requirement that the f-sum rule for the effective number of target electrons participating in the target excitations shall be satisfied. This procedure has proven [25] to give a quite accurate description of the target energy loss spectra in a wide range of momentum and energy transfers.

The values of the parameters appearing in eq. (4) that fit the energy loss function of amorphous carbon [26] are $A_1 = 0.0125$, $\omega_1 = 0.23$ au, $\gamma_1 = 0.21$ au, $A_2 = 0.633$, $\omega_2 = 0.945$ au, and $\gamma_2 = 0.49$ au. In this way we reproduce the two peaks in the loss function found experimentally [26] at $\sim$ 6 eV and $\sim$ 26 eV, which describe, respectively, the collective excitations of π and $\pi + \sigma$ electrons in amorphous carbon.

The above procedure should suffice if it is considered that the internuclear distances do not change as the molecule moves through the foil. But due to repulsion between the protons that form the molecule, the internuclear distances change while the molecule travels through the foil. The calculation of internuclear separations as a function of time, due to repulsion, cannot be done analytically for the H_3^+ molecule, as was for the simpler case of H_2^+ [4]-[6], therefore we have solved numerically the set of Newton equations of the three-proton system considering that each pair of protons separated at a distance r interact through the screened Coulomb potential [27] $V(r) = Z_{\rm p}^* \, r^{-1} \exp[-r/a]$, where $a = v/\omega_{\rm pl}$ is the dynamic screening length due to the screening of the valence electrons in the target. In the case of amorphous carbon, $\omega_{\rm pl}$ corresponds to the plasma resonance peak of higher energy, that is $\omega_{\rm pl} = 0.945$ au.

The effect of the screened Coulomb repulsion is to increase each side of the H_3^+ equilateral triangle, without changing its shape. Taking the initial time, $t = 0$, when the molecule enters the foil with the mean equilibrium internuclear distance $r_0 = r(t = 0) = 1.89$ au [21], fig. 1 shows how the internuclear distance between each couple of protons in the H_3^+ molecule changes as a function of time, $r(t)$, for two velocities, $v = 1$ au and $v = 2$ au, which cover the range of the experimental situation to be discussed later on; the case of Coulomb repulsion without screening is also depicted as a dotted line. It can be seen that not including screening would give a significant difference in the time-dependent internuclear distance for long times, which correspond to thicker foils. This difference diminishes as the molecule velocity increases. At low velocities the screening is stronger because the valence electrons of carbon are fast enough to screen the charge of the protons.

The stopping power $S_{H_3^+}^{\rm foil}$ of the H_3^+-molecule ion after traversing a foil with thickness d was evaluated as the time average of the instantaneous stopping power $S_{H_3^+}(r(t))$ corresponding to each internuclear distance r. Then eqs. (1) and (3) were used taking into account the variation of r with t due to the screened Coulomb interaction:

$$S_{H_3^+}^{\rm foil} = \frac{1}{\tau} \int_0^\tau {\rm d}t \, S_{H_3^+}(r(t)) \, , \tag{5}$$

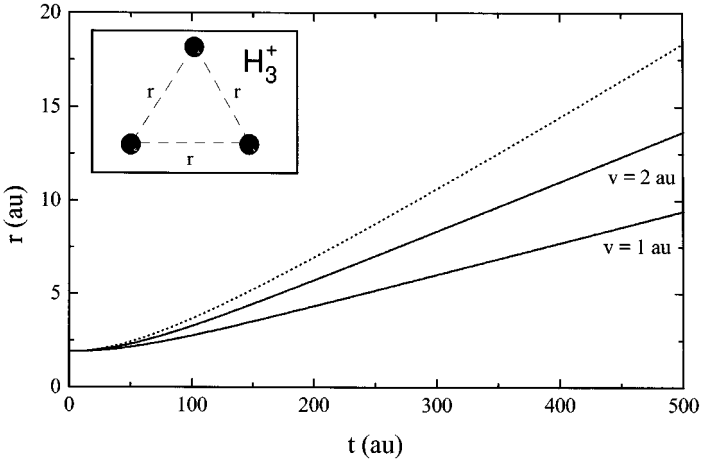

Fig. 1. – Instantaneous internuclear distance of the protons, which constitute the H_3^+ molecule, as a function of travel time. The dotted curve corresponds to the case of a pure Coulomb explosion. The solid curves incorporate the effect of electronic screening to the Coulomb repulsion for two different projectile velocities. The inset shows the H_3^+ molecule geometry.

where τ is the molecule dwell time, given by $\tau = d/v$ assuming that the molecule velocity does not change appreciably when traversing the foil.

Note that our model is not restricted to cases in which the H_3^+ molecular ions are transmitted through the foil, but it includes cases where the three separate fragments are detected.

Results and conclusions. – Figure 2 depicts the energy loss ratio $S^{\rm foil}_{H_3^+}/3S_{\rm p}$ of a randomly oriented H_3^+-molecule beam as a function of the amorphous carbon foil thickness and for the incident projectile energies 60, 80, 100 and 120 keV/amu, where experimental data are available. Due to the uncertainties in the amorphous carbon density, depending on the experimental methods used to prepare the samples and to measure their density [28], we have represented our calculations corresponding to 1.7 g/cm^3 (dotted line) and 2 g/cm^3 (solid line), although it can be appreciated that the differences only take place at intermediate thickness and are not sizeable. It can be noted that, in the range of energies considered in this paper, the vicinage effects are always positive and increase with the incident energy of the H_3^+ molecule. Therefore an enhacement in the H_3^+-molecule stopping power is found in comparison with that of three uncorrelated protons.

As the foil thickness (or, equivalently, the dwell time) increases the stopping power ratio decreases and tends to a constant value, indicating that vicinage effects take place only at the beginning of the molecule journey inside the target. This is because the distance among the protons increases with time, due to Coulomb repulsion, and when the separations become large compared with $v/\omega_{\rm pl}$, the individual proton fragments are not influenced by the wakes created by their partners. For short dwell times, the internuclear separations are small (compared to $v/\omega_{\rm pl}$), so the molecule acts like a point charge, $Z^2_{H_3^+} \simeq (\sum Z_{\rm p})^2$, as far as distant collisions with target electrons are concerned, while it acts like a collection of separate protons: $Z^2_{H_3^+} \simeq \sum(Z^2_{\rm p})$, with respect to energy transfers in close collisions.

The comparison with the available experimental data [19] included in fig. 2 shows a very good agreement for the full range of foil thicknesses and projectile energies covered by the

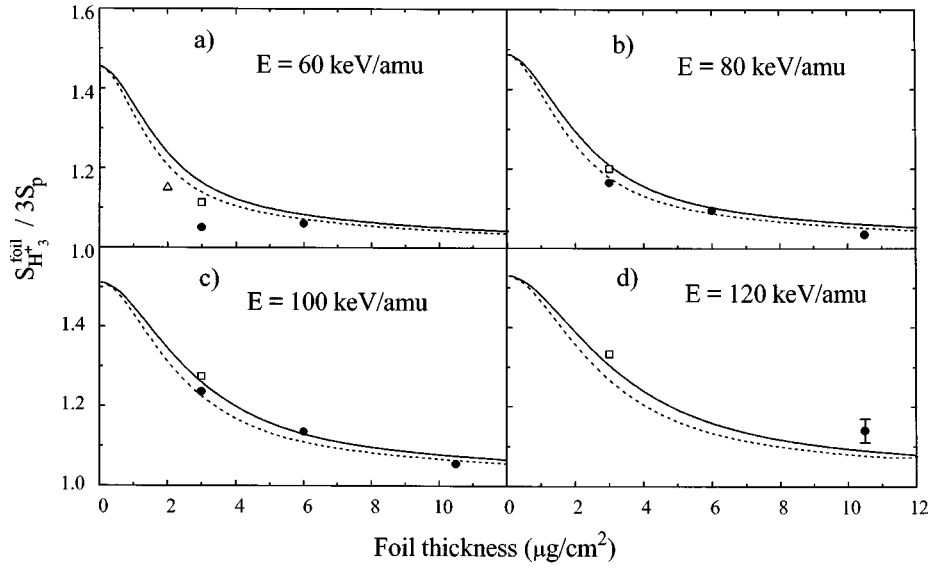

Fig. 2. – Comparison of calculated and experimental stopping power ratios corresponding to four different projectile energies: *a*) 60 keV/amu, *b*) 80 keV/amu, *c*) 100 keV/amu, and *d*) 120 keV/amu. Solid line: our calculations using a density 2 g/cm^3 for the amorphous carbon foil; dotted line: *idem* with 1.7 g/cm^3; full circles: experiments by Ray *et al.* [19]; open squares: calculations by Ray *et al.* [19], and open triangle: Monte Carlo simulation [10].

experiments. Our results also compare fairly well with other theoretical estimates [10], [19] shown in fig. 2. It is worth noting that our model can account for the allotropic or phase effects that characterize the aggregation state of a target, as is the case of carbon, which can be obtained as diamond, graphite, amorphous or C_{60}, showing quite different properties. On the other hand, for the wide range of foil thicknesses and projectile energies of experimental interest, Monte Carlo calculations [10] would require large computation times to include detailed target and molecule characteristics.

In conclusion, a formalism has been presented to calculate the stopping power of swift H_3^+ molecules in solids. The dynamics of the cluster fragments (Coulomb explosion) during their transit through the foil is included in the model, and the mean energy loss of the transmitted particles is evaluated by an average over the dwell time of the instantaneous stopping power. One of the main advantages of the present approach lies in the use of a dielectric-function formulation based on Mermin-type functions. This provides a more realistic description of the response function and energy absorption properties of specific materials. In this way, the present model takes into account the target properties in an accurate, although simple, manner.

***

We acknowledge partial support from the Spanish DGICYT (projects PB92-0341 and PB93-1125). NRA is a visiting professor under the program PROPIO (Conselleria d'Educació i Ciéncia de la Generalitat Valenciana). CD thanks the Instituto de Cooperación Iberoamericana for a doctoral fellowship.

REFERENCES

[1] Gras-Martí A., Urbassek H. M., Arista N. R. and Flores F. (Editors), *Interaction of Charged Particles with Solids and Surfaces, NATO ASI Ser. B*, **271** (Plenum, New York, N.Y.) 1991.

[2] *Proceedings of the Conference on Polyatomic Ion Impact on Solids and Related Phenomena* (*Saint Malo, 1993*), in *Nucl. Instrum. Methods B*, **88** (1994) 1 and ff.

[3] Caruso A. and Sindoni E. (Editors), *Proceedings of the International School of Plasma Physics on "Inertial Confinement Fusion"* (Editrice Compositori, Bologna) 1988.

[4] Brandt W., Ratkowsky A. and Ritchie R. H., *Phys. Rev. Lett.*, **33** (1974) 1325.

[5] Arista N. R., *Phys. Rev. B*, **18** (1978) 1.

[6] Gemmell D. S., *Chem. Rev.*, **80** (1980) 301.

[7] Steuer M. F. and Ritchie R. H., *Nucl. Instrum. Methods B*, **33** (1988) 170; **40/41** (1989) 372.

[8] Vager Z., Naaman R. and Kanter E. P., *Science*, **244** (1989) 426.

[9] Arista N. R. and Gras-Martí A., *J. Phys. Condens. Matter*, **3** (1991) 7931.

[10] Farizon M., de Castro Faria N. V., Farizon-Mazuy B. and Gaillard M. J., *Phys. Rev. A*, **45** (1992) 179.

[11] Wang Y. and Ma T., *Phys. Lett. A*, **178** (1993) 209.

[12] Jakas M. M. and Capuj N. E., *Phys. Rev. A*, **52** (1995) 439.

[13] Kaneko T., *Phys. Rev. A*, **51** (1995) 535.

[14] Eckardt J. C., Lantschner G., Arista N. R. and Baragiola R. A., *J. Phys. C*, **11** (1978) L851.

[15] Laubert R., *IEEE Trans. Nucl. Sci.*, **NS-26** (1979) 1020.

[16] Susuki Y., Ito T., Kimura K. and Mannami M., *Nucl. Instrum. Methods B*, **61** (1992) 3535.

[17] Susuki Y., Fritz M., Kimura K., Mannami M., Sakamoto N., Ogawa H., Katayama I., Noro T. and Ikegami H., *Phys. Rev. A*, **50** (1994) 3533.

[18] Fritz M., Kimura K., Susuki Y. and Mannami M., *Phys. Rev. A*, **50** (1994) 2405.

[19] Ray E., Kirsch R., Mikkelsen H. H., Poizat J. C. and Remillieux J., *Nucl. Instrum. Methods B*, **69** (1992) 133.

[20] Bohr N., *K. Dan. Vidensk. Selsk. Mat. Fys. Medd.*, **18**, No. 8 (1948).

[21] Gaillard M. J., Gemmell D. S., Goldring G., Levine I., Pietsch W. J., Poizat J.-C., Ratkowski A. J., Remillieux J., Vager Z. and Zabransky B. J., *Phys. Rev. A*, **17** (1978) 1797.

[22] Yarlagadda B. S., Robinson J. E. and Brandt W., *Phys. Rev. B*, **17** (1978) 3473.

[23] Abril I., Garcia-Molina R. and Arista N. R., *Nucl. Instrum. Methods B*, **90** (1994) 72.

[24] Mermin N. D., *Phys. Rev. B*, **1** (1970) 2362.

[25] Planes D. J., Garcia-Molina R., Abril I. and Arista N. R., to be published in *J. Electron Spectrosc. Relat. Phenom.* (1996).

[26] Cazaux J. and Gramari P., *J. Phys.* (*Paris*), **38** (1977) L133.

[27] Brandt W., in *Atomic Collisions in Solids*, edited by S. Datz, B. R. Appleton and C. D. Moak, Vol. **1** (Plenum, New York, N.Y.) 1975, p. 261.

[28] Stoner J. O., *Nucl. Instrum. Methods A*, **303** (1991) 94.